Local measurement of the zenithal anchoring strength

João G. Fonseca and Yves Galerne
Institut de Physique et Chimie des Matériaux de Strasbourg, Groupe des Matériaux Organiques, 23 Rue du Loess, 67037 Strasbourg, France
(Received 23 July 1999)

We present an electro-optic method for measuring the zenithal anchoring strength of nematic liquid crystals, based on the determination of the distortion produced by a small electric field. This method yields the zenithal anchoring strength at small applied torques, and remarkably, only needs local measurements (optical path difference versus applied voltage, sample thickness), in contrast to the classical methods that use measurements integrated over the entire sample. We determine the zenithal anchoring strength for two nematic liquid crystals (5 CB and 5 OCB) with positive dielectric anisotropy, onto poly(tetrafluoroethylene) (PTFE) treated surfaces, that yield planar liquid crystal cells. We find that the anchoring at the PTFE-5 CB interface is strong, with an extrapolation length ~30 nm, and independent of temperature far enough from the isotropic transition. We observe a pretransitional weakening of the anchoring strength near the nematic-isotropic transition, due to the reduction of the orientational order parameter at the interface. With 5 OCB, we measure a stronger anchoring, with an extrapolation length ~15 nm. This result may be explained by the increase of the van der Waals interactions between the liquid crystal molecules and the surface, due to the presence of the oxygen atom.

PACS number(s): 61.30.−v, 64.70.Md, 68.45.−v

I. INTRODUCTION

In the past few years, for fundamental reasons but also because of the potential display applications, there has been an increasing interest in studying the surface properties of liquid crystals and more specifically, their anchoring properties onto solid substrates. The preferred alignment directions of nematic liquid crystals (NLC) [1–3], and then the zenithal [4] and azimuthal [5–8] anchoring strengths, have thus been determined onto different substrates, essentially ITO glass plates coated with organic materials as polymer and amphiphilic molecules. Polymers such as polyamide [9,10] or PTFE [11] are found to produce the planar orientation (nematic director parallel to the surface) while amphiphilic molecules such as lecithin [12] or silane [13] yield the homeotropic orientation (perpendicular to the surface). Other techniques are more sophisticated and yield alignment layers with a wider range of anchoring properties. By means of oblique deposition of SiO coatings [14–17] one may observe a transition from the planar to the oblique anchorings as a function of the deposition angle. More recently, a nonmonotonic behavior of the anchoring properties of a monolayer deposited with the Langmuir-Blodgett technique, has been observed on varying its surface density [18]. Finally, with plasma modified silane monolayers, one observes an anchoring transition from the homeotropic to the planar anchorings at a critical density of the oxygen grafted onto the surface [19–21].

The zenithal anchoring strength is less frequently measured though this property is interesting in itself, and seems moreover particularly important for the recently discovered display mechanisms [22–25]. Usually, it is expressed in terms of the zenithal extrapolation length [26] ξ_θ, (see Sec. II A). Different experimental means are available to determine ξ_θ. Let us briefly recall them.

The wedge-cell method [27–29], initiated by Rivière *et al.*, uses a hybrid wedge-cell to measure the zenithal extrapolation length in one of the interfaces without needing to apply an external field. The major drawback of the method is that it needs a reference anchoring surface (assumed to be infinitely strong) to provide the conflicting boundary conditions. This naturally places an upper limit to the accessible anchoring strengths. Moreover, the method is excessively sensitive to defects and nonuniformities of the surface treatment, and works only with planar anchorings. So, since a few years, the methods which use an external electric field [30–47], seem more convenient, all the more than they are essentially close to the conditions encountered in the display devices.

Among several possible variations, two of the most common procedures based on applying an electric field, are the anchoring breaking method [44–47] and the high electric field technique [40,41]. Both methods use strong electric fields and measure the anchoring strength close to the maximum of the anchoring torques. In the anchoring breaking method, which may be performed on planar anchorings only, one applies a sufficiently high electric field to break the anchoring of the nematic from its easy axis onto the substrate. Then, and assuming equal elastic constants $K_{11}=K_{33}=K$, the extrapolation length and the electric coherence length, $\xi_E=(K_{11}/\varepsilon_0\varepsilon_\parallel)^{1/2}/E_c$, are equal $\xi_\theta \approx \xi_E$ [47]. By measuring the field E_c that produces the breaking of the anchoring (then the nematic is oriented homeotropically, and the cell exhibits a zero path difference between the ordinary and extraordinary rays in normal incidence), one can directly determine the extrapolation length. However, one may notice that, though it is not crucial, accurate determinations of E_c are not easy to realize, essentially because it is difficult to distinguish between a small path difference and a null one. Moreover, there are often problems at high electric fields, essentially because of electrolysis which irremediably produces ions. The electric field is then partly screened out, and disturbing flows appear in the sample. Such problems are even worse for strong anchorings since the applied electric field

have to be large in these cases.

In the high electric field technique, the zenithal extrapolation length ξ_θ is determined by exploiting a roughly linear regime of the optical path difference ratio $\delta(V)/\delta(V=0)$ versus $1/CV$, where C is the sample capacitance and V the applied voltage. Such a behavior may be shown from free energy minimization, and is valid for high enough voltages. Then, ξ_θ is determined from a linear extrapolation of the data. This method presents a wide voltage range of application, and can be performed on both planar and tilted anchorings [4], but it needs thick samples ($\sim$50 μm), much thicker than used for the display applications ($\sim$5 μm). It also needs complementary measurements as the measurements of the sample capacity. Experimentally, capacity measurements are integrated over the whole surface of the electrodes, so that the physical characteristics of the sample have to be uniform. In particular, the sample thickness and the surface treatment are required to be as uniform and homogeneous as possible. In practice, the uniformity conditions of the sample are rarely realized. This is a supplementary cause of experimental errors. Moreover, the capacity measurements are not really standard, since they have to be performed in the presence of the electric field, generally alternative, which produces the torque and therefore the distortion.

We propose here a local method for measuring the zenithal anchoring strength in the small torques limit, that therefore avoids the problems related to high electric fields and to the nonuniformity of the sample thickness or the surface treatment. Essentially, we determine the director distortion inside the sample on measuring the optical path difference as a function of the applied voltage above the Fredericks transition, in a small area of the sample. We then extrapolate the distortion out of the sample limits to deduce the extrapolation length and the zenithal anchoring strength.

II. PRINCIPLE OF THE LOCAL METHOD

Before entering into the details of our experimental procedure for measuring the anchoring strength, let us first quickly recall the relationship that exists between the nematic distortion, the extrapolation length, and the optical path difference in normal incidence. We then discuss the way to perform the calculations.

A. Free energy

We consider a sample of NLC with positive dielectric anisotropy ε_a, between two parallel substrates at $z=\pm d/2$, uniformly and identically treated, with parallel easy directions ($\varphi=0$). The NLC director in the cell is $\boldsymbol{n}=(\sin\theta,0,\cos\theta)$. Assuming translational symmetry in the horizontal plane, we restrict the problem to one dimension, $\theta\equiv\theta(z)$. We also assume that the NLC is perfectly insulating and that the anchoring is uniformly planar [$\theta_s=\theta(\pm d/2)=\pi/2$] in the absence of external fields. An electric field is then applied perpendicular to the surfaces. At low voltages, below the Frederiks threshold [48], the NLC keeps everywhere oriented along the **x** axis. For higher voltages than the threshold, one observes a distortion in the NLC cell as the nematic molecules tend to align along the electric field. If then the anchoring has a finite strength, the orientation of the director at the surface is no longer planar [$\Delta\theta_s \equiv \theta_s-\theta(\pm d/2)>0$]. One can then extrapolate the distortion from the real surface to a virtual one where the anchoring is once again planar and infinitely strong (Fig. 1). The distance between the two surfaces is defined as the zenithal extrapolation length ξ_θ. It is related, in first approximation [26], to the anchoring strength coefficient E_a, and to the bend elastic constant K_{33}, by the equation $\xi_\theta=K_{33}/E_a$.

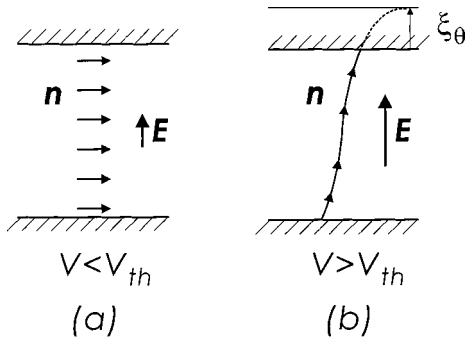

FIG. 1. Orientation of the nematic director in a liquid crystal cell with planar anchoring, for (a) Applied voltages smaller than Frederiks threshold. (b) Above threshold, the competition between the electric and the surface torques give rise to a distortion. In the case of finite anchoring strengths, the anchoring at the surfaces is no longer planar. The zenithal extrapolation length ξ_θ is defined as the distance between the real surface of the sample and a virtual one where the director is once again planar.

At a given applied voltage V, the director distortion $\theta(z)$ is determined from minimization of the free energy per unit area of the sample [26]:

$$F=\int_{-d/2}^{d/2}(f_{\text{elast}}+f_{\text{elect}})dz+2\,f_{\text{surf}}(\Delta\theta_s). \tag{1}$$

In this expression, f_{surf} is the coupling energy of the NLC to the substrate. Following Rapini and Papoular (RP) [49], f_{surf} may be approximated to the first order in the variations of the director orientation at the surfaces ($\Delta\theta_s\ll 1$) by

$$f_{\text{surf}}=\frac{1}{2}E_a\Delta\theta_s^2, \tag{2}$$

where E_a is the anchoring strength coefficient. Let us notice that the RP approximation is not very restrictive, since experimentally it is justified up to a wide range of angle variations, typically $\Delta\theta_s<\pi/6$ (see, for instance, Ref. [44]).

The electric energy density is given by the relation

$$f_{\text{elect}}=\frac{1}{2}\boldsymbol{D}\cdot\boldsymbol{E}=-\frac{1}{2}\frac{C^2V^2}{\varepsilon(\theta)}, \tag{3}$$

where $\varepsilon(\theta)=\varepsilon_0(\varepsilon_\parallel\cos^2\theta+\varepsilon_\perp\sin^2\theta)$, $\varepsilon_\parallel$ and $\varepsilon_\perp$ being the relative dielectric constants of the NLC for $\boldsymbol{E}$ parallel and perpendicular to $\boldsymbol{n}$, respectively. According to Maxwell's equations, the electric displacement $\boldsymbol{D}$ keeps constant over the whole sample and, since the electric field $\boldsymbol{E}$ has to be normal to the electrodes, its orientation is in general not along z. Its z component is related to the electric potential V by the relation $D_z=CV$, where C is the sample capacity per unit area:

$$C=\frac{1}{\int_{-d/2}^{d/2}\frac{1}{\varepsilon(\theta)}dz}. \tag{4}$$

Expression (4) is integrated over the whole distortion $\theta(z)$. As we shall see below, the exact expression of the distortion $\theta(z)$ can be calculated only numerically. The integration (4) has therefore to be performed numerically also, so that C and the electric energy (3) cannot be determined exactly before the distortion is known. Practically, we proceed with the calculation of the distortion in at least two steps. In the first one, we neglect the sample distortion and approximate the electric energy on considering that the electric field is constant inside the cell, and simply equal to V/d. In this manner, we get a first approximation of the NLC distortion that we use in a further step to calculate C and the electric energy, more correctly.

Due to our particular experimental conditions, the distortion involved in the sample is limited to the **xz** plane, with only splay and bend contributions. The elastic energy density may then be expressed as

$$f_{\text{elast}}=\frac{1}{2}K(1-\chi\cos 2\theta)\left(\frac{\partial\theta}{\partial z}\right)^2, \tag{5}$$

where $K=(K_{11}+K_{33})/2$, $\chi=(K_{11}-K_{33})/2K$, K_{11} and K_{33} being the splay and bend elastic constants of the NLC. Note that the surfacelike splay-bend elastic term in K_{13} is not included here in the elastic energy density since, as recently shown [50,51] this term does not exist in fact. Several arguments have been proposed to justify that K_{13} is zero. In particular, this elastic coefficient would surprizingly lead to a distorted ground state of the NLC cell in the absence of any applied field. The surfacelike saddle-splay elastic term with the K_{24} coefficient is also null here due to the one-dimensional nature of the problem.

B. Determination of the NLC distortion

We may now minimize free energy (1) and calculate the equilibrium distortion in the cell submitted to an electric field $\boldsymbol{E}$. Before doing this, let us notice that the distortion above the Frederiks threshold, is symmetric because of the symmetry of both the cell and the field, so that $\theta(z)=-\theta(-z)$. The calculations may therefore be restricted to the domain $z\in[0,d/2]$. For practical reasons, we choose to start the integration from the center of the cell (at $z=0$). The anchoring strength onto the surfaces being unknown at this stage, boundary conditions have to be assumed to perform the calculation of the distortion. We thus choose the starting value of the angle at the center of the cell, to be $\theta(0)=\theta_0$. Following the usual method, the integration is performed in two steps. First the Euler-Lagrange equation is obtained and integrated to yield

$$\frac{\partial\theta}{\partial z}=\left(\alpha(\theta)B\frac{\cos^2\theta_0-\cos^2\theta}{1-\chi\cos 2\theta}\right)^{1/2}, \tag{6}$$

where B and $\alpha(\theta)$ are defined as

$$B=\frac{\varepsilon_0(\varepsilon_\parallel-\varepsilon_\perp)V^2}{Kd^2},\quad \alpha(\theta)=\frac{C^2d^2}{\varepsilon(\theta_0)\varepsilon(\theta)}. \tag{7}$$

The boundary condition at $z=d/2$ is given by

$$\frac{df_{\text{surf}}}{d\theta}=K(1-\chi\cos 2\theta)\left.\frac{d\theta}{dz}\right|_{z=d/2}, \tag{8}$$

which expresses the torque equilibrium at the surface of the substrate.

The distortion $\theta(z)$ is then obtained on integrating the differential equation (6). This second integration cannot be performed analytically, only numerically, and as discussed above, we start the calculation from the center of the cell with the tilt angle θ_0. However, due to symmetry, the cell center is an inflexion point in the ***n***-field line, which imposes the condition $d\theta/dz|_{z=0}=0$. This relation clearly prevents us to prime the numerical calculation directly from Eq. (6). To escape the problem, we start the integration by means of an expansion of Eq. (6) valid close to $z=0$. The distortion may then be calculated to the lowest order in z as

$$\theta(z)=\theta_0+\frac{1}{4}\frac{\alpha(\theta_0)B\sin 2\theta_0}{1-\chi\cos 2\theta_0}z^2. \tag{9}$$

Then, as soon as $|d\theta/dz|$ is sufficiently different from zero, the numerical integration of Eq. (6) can begin normally. Practically, expression (9) is used in the range $|\theta(z)-\theta_0|<10^{-4}$ rad only.

Let us notice that, due to the distortion, a flexoelectric coupling arises between the applied electric field and the polarization induced by the distortion. This flexoelectric effect cannot be introduced in the first run of the calculation, since the distortion is unknown yet. This is done in the further runs by means of a renormalization of the elastic constant, according to the expression [52]

$$K(\theta)=(K-\delta K\cos 2\theta)+\frac{(e_1+e_3)^2}{4\varepsilon(\theta)}\sin^2 2\theta, \tag{10}$$

where e_1 and e_3 are the flexoelectric constants of the NLC. So, because the two corrections $\alpha(\theta)$ in Eq. (6) and $K(\theta)$ are *a priori* unknown, the calculation of the distortion needs several numerical runs. The calculations are thus performed in a loop, until the distortion stabilizes within an accuracy of at least 10^{-3} rad in the tilt angle onto the substrate $\theta_{d/2}$.

C. Zenithal extrapolation length

Once the exact distortion $\theta(z)$ is calculated, we determine the zenithal extrapolation length ξ_θ, on simply continuing the calculation of the distortion in the range $z>d/2$, but with zero electric field, until z^* where the director retrieves the initial orientation at the surface, $\theta(z^*)=\theta_s$. According to definition, the extrapolation length is $\xi_\theta=z^*-d/2$. One may equivalently determine ξ_θ on writing the equilibrium condition between the surface and the volume torques. Equating the surface torque, $\Gamma_S=E_a\Delta\theta_s$ in the *RP* approximation, and the volume torque Γ_v, obtained on integrating the electric torque

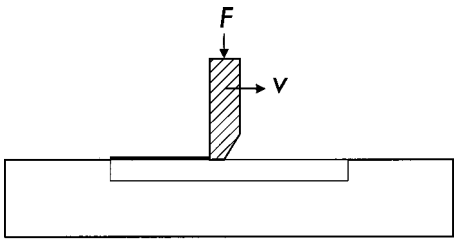

FIG. 2. A PTFE bar (hatched) is rubbed on an ITO coated glass plate at a speed $v \sim 0.2$ mm/s, temperature $\sim 230\,^{\circ}$C, and with a pressure $\sim$ 10 bar. A thin PTFE film (thick line) is deposited in this way with most of its fluorinate chains aligned along the friction direction.

$$\Gamma_V = \int_0^{d/2} |\boldsymbol{P}\cdot\boldsymbol{E}|\,dz = \int_0^{d/2} \frac{1}{2}\,\alpha(\theta) B K(\theta)\,\frac{\varepsilon(\theta_0)}{\varepsilon(\theta)}\sin 2\theta\, dz, \tag{11}$$

we finally deduce the zenithal extrapolation length:

$$\xi_\theta = \frac{2K_i \Delta\theta_s}{B\int_0^{d/2}\alpha(\theta)K(\theta)\,\dfrac{\varepsilon(\theta_0)\sin 2\theta}{\varepsilon(\theta)}\,dz}. \tag{12}$$

Knowing the distortion inside the cell, we may now calculate the optical path difference δ_{calc} between the ordinary and the extraordinary rays that pass through the sample. In normal incidence and for our planar distortion, restricted to the ***xz*** plane, the Maxwell's equations yield the usual expression, which is therefore exact contrarily to what in sometimes asserted [4] (see the Appendix):

$$\delta_{\mathrm{calc}} = \int_{-d/2}^{d/2}\left(\frac{n_0 n_e}{\sqrt{n_0^2\sin^2\theta + n_e^2\cos^2\theta}} - n_0\right) dz, \tag{13}$$

In this manner, and with the help of some NLC physical parameters such as the optical indices and the elastic constants, we get the optical path difference δ_{calc} as a function of the angle θ_0 chosen in the center of the cell. By comparison to the measured optical path difference δ_{expt}, we finally determine the distortion of the NLC cell and the extrapolation length at the surfaces, as functions of the applied voltage V.

III. EXPERIMENTS

A. Samples

Poly(tetrafluoroethylene) (PTFE) films are deposited on ITO coated glass plates (square resistance $\leqslant 100\ \Omega$, thickness $\sim$25 nm) by means of hot friction (Fig. 2), following the procedure developed by Wittman and Smith [53]. The deposition is made twice in order to assure a good uniformity of the alignment. Measurement cells are then prepared, with the two plates in the parallel (or indifferently anti-parallel) azimuthal orientation. Silica spheres of $\sim 5\ \mu$m are used as spacers in-between, and an effective surface ~ 1 cm^2 is left for the NLC sample. The parallelism of the plates is carefully adjusted by controlling the pressure exerted by four screws at the corners of the cell, and by observing the equal-thickness interference fringes with Hg light [11]. Epoxy glue is then used to permanently fix the cell plates. The sample cells are placed in an electric thermostat (from Instec) in which the temperature is stabilized to within $\sim$10 mK. The liquid crystal is introduced in the cell by capillarity in the isotropic phase and heated up at $\sim$15 K beyond the nematic-isotropic transition, to avoid parasitic memory effects onto the anchoring, due to the shear flows produced during the cell filling. Uniformly oriented nematic cells are obtained with this procedure (Fig. 3). They exhibit a planar anchoring with an azimuthal orientation parallel to the PTFE friction direction, as already reported for this type of surface [11].

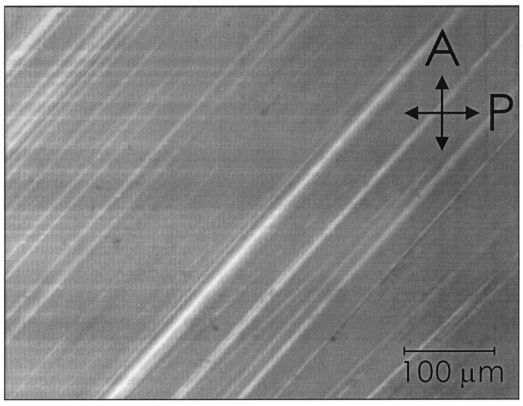

FIG. 3. Typical photograph of a 5 CB sample between crossed polarizers (*A* and *P*). The orientation is uniformly planar with, however, stripes along the rubbing direction that probably correspond to different thicknesses in the PTFE layer.

We perform the anchoring measurements with two resembling compounds, 5 CB(4-cyano-4′-*n*-pentylbiphenyl) and 5 OCB(4-cyano-4′-*n*-pentyloxybiphenyl), to test the effect on the anchoring properties, of the oxygen atom located about in the middle of the molecule (Fig. 4). Both compounds are cyanobiphenyls with strong positive dielectric anisotropies, which make them easy to align with an electric field. The temperatures of the nematic-isotropic transitions are $T_{N-I} = 34.5\,^{\circ}$C for 5 CB $T_{N-I} = 67.5\,^{\circ}$C for 5 OCB. One commonly observes narrow birefringent stripes ($\sim 10\ \mu$m large) parallel to the PTFE deposition direction under polarizing microscope. These stripes are not visible before introducing the NLC, and typically persist up to $\sim$15 K above the nematic-isotropic transition. They correspond to scratches in the PFTE film with probably a reduced thickness. The fact that they persist at temperatures above the nematic-isotropic

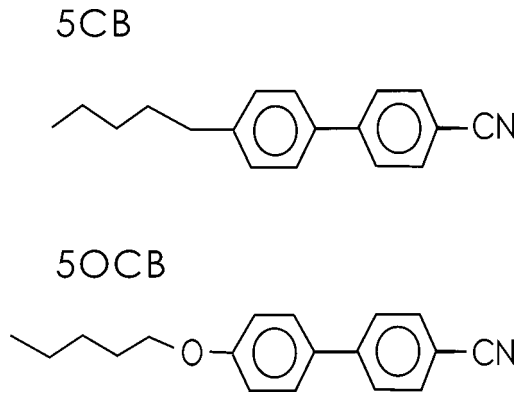

FIG. 4. 5 CB and 5 OCB molecules. They differ from each other by only one oxygen atom.

transition seems to indicate that the nematic contact layer is highly ordered in these places, and that it needs a stronger entropy to go in the isotropic phase.

B. Parameters

In order to determine the zenithal extrapolation length (Sec. II), one first measures the optical path difference δ_{expt} in a uniformly oriented nematic cell (Sec. III A) as a function of the applied voltage V. One then calculates the distortion in the cell and for that, one has to know several physical parameters with an equilibrated precision. From a sensibility study of ξ_θ on the different physical parameters, we observe that they are not all equally important for the quality of the measurement. We thus select a group of nonsensitive parameters, which are the relative dielectric constants $\varepsilon_\parallel$ and $\varepsilon_\perp$, the ordinary optical index n_0, the ratio of the NLC elastic constants K_{33}/K_{11}, and the flexoelectric constant e_1+e_3. These parameters can just be taken from literature [54–59]. For example, for 5 CB at a temperature $\Delta T=7.5$ K below the isotropic transition, we find $\varepsilon_\parallel=10.72$, $\varepsilon_\perp=7.05$, $n_0=1.54$, $K_{33}/K_{11}=1.53$, $e_1+e_3=5\times10^{-10}\,\text{Cm}^{-1}$.

At the opposite, the other parameters of the cell (the sample thickness, the NLC birefringence, the anchoring tilt and the ratio K_{11}/ε_a) which play a predominant role in the calculation of the distortion, have to be determined all the more carefully than their relative errors propagate to the extrapolation length with an amplification factor of 2 to 3. The thickness of the empty cells is measured after solidification of the glue, with a precision ~0.1 μm, by measuring the distance between the Michelson-like interference fringes produced by a He-Ne laser beam diffused close to the cell [11]. Typical thicknesses are in the range of 5–10 μm, so that d is known to within a relative error $\Delta d\sim1-2$ %. The NLC birefringence and the anchoring tilt angle θ_s are determined in each cell before applying the electric field, by means of interferometry measurements equivalent to conoscopy [11]. The measurements are performed in the same experimental conditions (temperature, NLC, surface treatment) as the electro-optic measurements themselves, to reduce the experimental errors which typically are $\sim1°$. The ratio K_{11}/ε_a, which directly measures the elastic torque relative to the electric one, is particularly sensitive, and needs to be carefully determined. It may be deduced from the measurement of the Frederiks threshold V_{th}, through the relation, valid for planar strong anchorings, $V_{\text{th}}=\pi(K_{11}/\varepsilon_a)^{1/2}$. More generally, it may be obtained from a stability criterion concerning the variations of the extrapolation length with voltage (Sec. III D).

C. Electro-optic measurements

The optical path difference δ_{expt} is measured in white light by means of a tilting compensator (Leica), as a function of the ac applied voltage at frequency $f=10$ kHz. A capacity filter is placed in the circuit in order to suppress parasitic dc voltages from the ac signal, and to avoid electrolysis effects.

In Fig. 5(a) are shown typical measurements of the optical phase difference δ_{expt} as a function of the r.m.s. voltage V (for the 5 CB-PTFE interface at $\Delta T=7.5$ K). One can see the Frederiks transition and the associated rapid decrease in the optical phase difference with voltage. This behavior is completely reversible and exhibits no hysteresis. One also observes that the transition is not as well defined as in theory. The slope at transition in Fig. 5, clearly differs from vertical. This difficulty in determining the Frederiks threshold directly, has already been reported by different authors [60,61]. In our case, it is probably due to local variations in the director orientation which are induced by substrate irregularities as mentioned above about the birefringent stripes. Although the measurements of the optical path differences are taken in a region as far as possible from the stripes, between two of them, they nevertheless can slightly be affected close to the transition because the sample there becomes critically sensitive to small perturbations. In a first attempt to avoid such a difficulty in determining the voltage threshold V_{th} accurately, one may fit a parabolic law, characteristic of the second-order mean-field transitions as generally are the Frederiks transitions, onto the experimental data as shown in Fig. 5(b). However, though improved, the V_{th} measurements obtained in this manner, do not generally lead to precise determinations of the anchoring strengths.

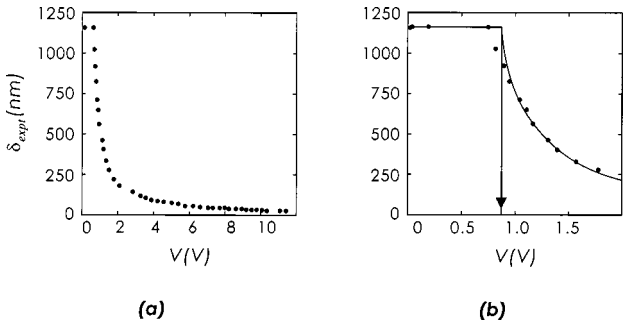

FIG. 5. Optical path difference δ_{expt} as a function of the applied voltage. The Frederiks transitions are generally not well defined and often appear to be smoothed a little bit with nonvertical slopes at $V=V_{\text{th}}$. (a) General view. (b) Zoom at the transition region. A fit of a power law with a $\frac{1}{2}$ exponent (solid line), is performed onto the experimental data to get a better determination of the threshold (arrow).

D. Criterions for V_{th} determination

To determine the parameter V_{th} with a better accuracy, we therefore prefer to use a simple criterion, based on the analysis of the variations of the calculated extrapolation length versus the applied voltage. In the RP approximation, which is valid at least for not too large tilt changes onto the substrate, $\Delta\theta_s$, the anchoring coefficient E_a is a constant. The zenithal extrapolation length $\xi_\theta(=K_{11}/E_a)$ should therefore be independent of the applied torques, i.e., of the applied electric field. As shown in Fig. 6, the calculated extrapolation lengths $\xi_\theta(V)$ exhibit variations with voltage which depend on the threshold value V_{th} chosen for the calculations. On selecting the value which yields an extrapolation length roughly independent of V, we determine the Frederiks threshold V_{th} (i.e., equivalently the ratio K_{11}/ε_a) and consequently, the extrapolation length ξ_θ, with a better accuracy.

In the case of planar anchorings, the above criterion may be presented differently. Due to symmetry, the extrapolation length is then an even function of the tilt change onto the substrate $\Delta\theta_s$, i.e., at the lowest order, ξ_θ is a constant, independent of V. Moreover, in the RP approximation, the

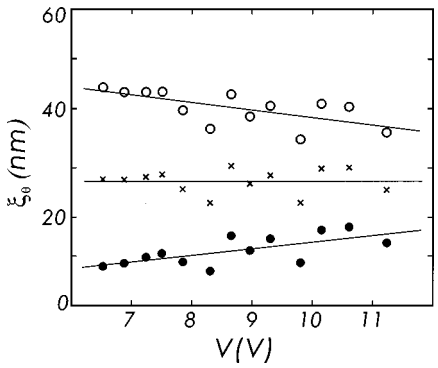

FIG. 6. Zenithal extrapolation lengths calculated with different values of the Frederiks voltage $V_{\rm th}$ ($V_{\rm th}=0.67$, 0.74, and 0.81 V, close dots, crosses, and open dots, respectively), as functions of the applied voltage for the 5 CB-PTFE interface at $\Delta T=7.5$ K. They exhibit positive (negative) variations with the applied voltage, depending on the too high (low) $V_{\rm th}$ values chosen for the calculations. Noticing that, in the RP approximation, the extrapolation length should be independent of the applied voltage, we deduce a simple criterion for determining the correct value for $V_{\rm th}$, and consecutively, for the zenithal extrapolation length. Here $\xi_\theta=30\pm5$ nm.

tilt change at the interface $\Delta\theta_s$ being proportional to the total electric torque, is also proportional to E^2 times the correlation length ($\xi_E\sim1/E$), i.e., $\Delta\theta_s$ is simply proportional to the applied electric voltage. In Fig. 7 are shown the tilt changes onto the substrate $\Delta\theta_s$ versus the applied voltage. They are calculated from the experimental data of Fig. 5, with the same threshold voltages as in Fig. 6, $V_{\rm th}=0.67$, 0.74, and 0.81 V (close dots, crosses, and open dots, respectively). The data in the vicinity of the Frederiks transition are excluded to avoid the systematic errors denoted above. The solid lines depict the linear least squares fittings in the three cases, respectively. Clearly, within the experimental errors, the intermediate value $V_{\rm th}=0.74$ V yields proportionality variations between $\Delta\theta_s$ and V, while the two others do not. Such behaviors are consistent with the above discussion, and may be used as a variant criterion for determining the threshold value $V_{\rm th}$ or the ratio K_{11}/ε_a, in the case of planar anchorings.

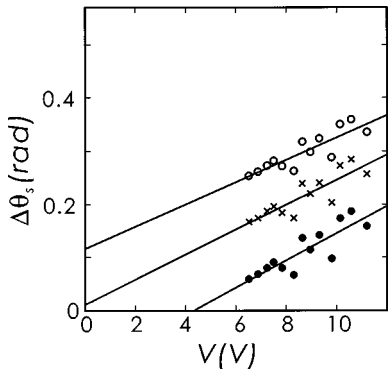

FIG. 7. Tilt changes onto the substrate, $\Delta\theta_s$, calculated for the experimental data of Fig. 5, as functions of the applied voltage with $V_{\rm th}=0.67$, 0.74, and 0.81 V (close dots, crosses, and open dots, respectively), and least-squares fits of linear behaviors (solid lines).

E. Experimental discussions

A total compensation of the path difference due to the sample, is easily achieved in the first order of the interference, simultaneously for all visible wavelengths. One then observes a precise black fringe. The path difference is thus measured with a precision of ~1 nm, i.e., with a relative accuracy better than 5%, except close to the anchoring breaking region where the optical path difference gets null. In the case of higher optical path differences which are obtained for thick samples at low voltages, one observes higher orders of interference. Unfortunately then, the dispersion properties of the NLC and of the compensator are different. The fringes are colored and thick, and the compensation tuning which slightly depends on the wavelength, cannot be realized accurately. To solve the problem, one could use color filters, but then, the light becomes insufficient to make good measures. So, we choose to determine the extrapolation length in the first interference order only. This also makes us to avoid the critical region of the Frederiks transition, where the sensitivity of the sample diverges and increases the experimental errors.

Another source of problems in the electro-optic measurements, arises from the ions that the nematic medium generally contains. At large concentrations, they can screen the electrodes from the applied electric field. The electric field effectively received inside the nematic cell, is then reduced and difficult to estimate. In such a case, the measurements of the anchoring strength should be erroneous. However, we may consider that the screening effect of the ions in the cell is negligible if the Debye length L_D is larger than the sample thickness d. The Debye length for monovalent ions is given by the relation

$$L_D=\sqrt{\frac{\varepsilon_0\varepsilon kT}{2ne^2}}, \tag{14}$$

where k is Boltzmann constant, T is the temperature, e is the electronic charge, and n the ion density. Knowing the ion mobility μ in the NLC (in the case of 5 CB, $\mu=3.5\times10^{-6}\,{\rm cm^2\,V^{-1}\,s^{-1}}$ [62]) and measuring the NLC resistivity ρ, one determines the ion density, using the relation

$$n=n_0\frac{kT}{2eV}=\frac{kT}{2\rho e^2\mu}. \tag{15}$$

Typically, we have $n_0\approx0.4\,{\rm mol/m^3}$ and a Debye screening length $L_D\sim15\,\mu{\rm m}>d$. For example, for a sample thickness of 7.5 μm, this corresponds to a reduction of the electric field inside the cell of $\sim$ 1%, and thus to a negligible screening effect. So, our samples may be considered to be in the pure dielectric regime. In the opposite case ($L_D\leqslant d$), one should have to make corrections corresponding to the conduction regime [52].

F. Experimental results

We measure the zenithal extrapolation length of the 5 CB-PTFE and PTFE-5 OCB interfaces at different temperatures, using the method described above. On the 5 CB-PTFE interface far from the nematic-isotropic transition, the zenithal extrapolation length is found to be rather small, ξ_θ

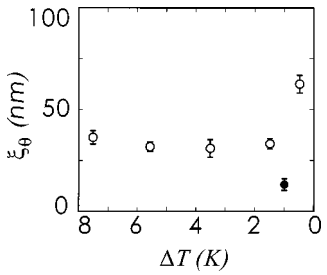

FIG. 8. Zenithal extrapolation length as a function of temperature for the 5 CB-PTFE interface (open dots). The anchoring strength is found to be strong and independent of temperature, except close to the nematic-isotropic transition where it noticeably decreases (larger ξ_θ). The anchoring strength is about twice larger at the 5 OCB-PTFE interface (close dot).

$=30\pm5$ nm, which corresponds to an anchoring strength coefficient $E_a \approx 10^{-5}$ J/m^2. These values indicate that the anchoring strength of 5 CB onto PTFE is similar as on SiO [41] (60 nm thick film deposited at an incidence angle of 60°), and twice as strong as on plasma modified silane, far from the homeotropic to planar transition [21]. The same measurements are repeated as functions of temperature. They indicate that except close to the nematic-isotropic transition, the anchoring keeps roughly independent of temperature (Fig. 8). When approaching to the nematic-isotropic transition on increasing temperature, one observes a quasicritical weakening of the anchoring strength. This pretransitional behavior of the anchoring strength has already been reported on other interfaces [14,41], and is probably due to the decrease of the orientational order parameter at the interface.

The same measurements performed at the 5 OCB-PTFE interface exhibit similar behaviors, but with a twice stronger anchoring strength. Far from the nematic to isotropic transition, the zenithal extrapolation length is measured to worth only $\xi_\theta = 15$ nm. Such a behavior is consistent with the remark that the extra oxygen atom increases the dipole moment and the polarizability of the 5 OCB molecules, and therefore reinforces their van der Waals and London interactions to the substrate. Though a minor change in the molecular skeleton, the supplementary oxygen atom is thus able to change the anchoring strength by a factor as large as 2. These measurements of strong zenithal anchorings of nematic liquid crystals onto PTFE alignment layers, confirm the qualitative observations previously reported by different authors [63,64].

IV. CONCLUSIONS

A local method for measuring the zenithal anchoring strength is proposed. The method is essentially based on the measurement of optical path differences across a NLC cell submitted to different applied voltages, and on the calculations of the subsequent distortions. Only a few physical parameters of the NLC cell, the sample thickness, the NLC birefringence, the anchoring tilt and the ratio K_{11}/ε_a, have to be known accurately to calculate the distortions correctly, and consequently to determine the zenithal anchoring strength. In principle, the measurements of the optical path differences can be performed satisfactorily in a wide range of voltages, from the Fredericks to the anchoring breaking transitions. However, in order to limit the electrolysis effects and to preserve the sample from pollution with too many ions, it is better to avoid the region of the high electric fields. If the voltage is restricted to low values enough for the RP approximation be valid (which roughly corresponds to the condition $\Delta\theta_s < \pi/6$), one may at the same time, take profit of a second advantage. One may then directly determine one of the most sensitive parameters, the ratio K_{11}/ε_a, by using the criterion of a constant extrapolation length calculated as a function of V, or equivalently by testing the proportionality of the tilt change onto the substrate $\Delta\theta_S$, with V (Sec. III D).

The measurements of the zenithal extrapolation lengths for the 5 CB-PTFE and 5 OCB-PTFE interfaces both indicate strong anchoring strengths far from the nematic-isotropic transition, with respectively, $\xi_\theta = 30\pm5$ nm and $\xi_\theta = 15\pm5$ nm for the 5 CB-PTFE and 5 OCB-PTFE interfaces. The zenithal anchoring strengths are found to be independent of temperature, except close to the nematic-isotropic transition where a pretransitional behavior is observed. More remarkably, the presence of an oxygen atom in the core of the NLC molecule enhances the anchoring strength, probably due to the enhancement of its van der Waals and London interactions with the PTFE substrate.

In conclusion, the method presented here for measuring the zenithal anchoring strengths may be compared with benefit to the other available types of measurements, the anchoring breaking method, the wedge-cell technique, the Frederiks transition technique, and the high electric field technique. Although the method described here, is a less direct method (it requires a PC program to determine the NLC distortion and the knowledge of some of the NLC physical parameters), it has several advantages when compared to the other ones. Essentially, it is a local method, so that the results are not affected by inhomogeinities in the thickness or in the surface treatment of the cell. Furthermore, there is no need of measurements of capacitance under electric field, and there is no limitation on the sample thickness. Let us also notice that the method essentially weighs the surface torque, and that the limitation to the low voltages is not necessary. However, when the voltages are limited in order that the RP approximation be valid, the data analysis may substantially be simplified on using a stability criterion. The zenithal anchoring strength is then measured in the range of the small torques, complementary to the range of other known techniques (high electric field technique and anchoring breaking method) which work close to the anchoring breaking.

Let us finally remark that the method presented here may be extended to pretilted anchorings ($\theta_s \neq \pi/2$). In this case, the main features for determining the zenithal anchoring strength keep essentially the same, though the Frederiks transition does not exist any more. Its threshold cannot be used to determine the parameter K_{11}/ε_a. One may nevertheless apply the criterion of a constant zenithal anchoring length as a function of voltage (as in Sec. III C and Fig. 6), if one restricts the measurements to voltages low enough to keep in the range of the RP approximation.

ACKNOWLEDGMENT

João G. Fonseca thanks the Portuguese Government for Grant No. PRAXIS XXI BD/9178/96.

APPENDIX: LIGHT PATH DIFFERENCE IN NORMAL INCIDENCE

The expression for the optical path difference in normal incidence, Eq. (13), is generally obtained from a Jones matrix calculation, and is then considered [4] to be an approximation, only valid for $\lambda \ll \xi_E$. Let us stress here that, in fact, this equation is exact and valid for any value of ξ_E. It may be shown as follows.

The electromagnetic wave which propagates along z, may be written as

$$\{\boldsymbol{E},\boldsymbol{D},\boldsymbol{B}\}=\{\boldsymbol{E}_0,\boldsymbol{D}_0,\boldsymbol{B}_0\}\exp\{j[\Phi(z)-\omega t]\}, \tag{A1}$$

From the Maxwell equations, we deduce that it satisfies to the relation

$$\omega^2\mu_0 D_x-\left(\frac{\partial\Phi}{\partial z}\right)^2 E_x=0, \tag{A2}$$

where E_x is the x component of the electric field of light and $\boldsymbol{D}$ is the electrical displacement given by

$$\boldsymbol{D}=\varepsilon_0\varepsilon_\perp\boldsymbol{E}+\varepsilon_0\Delta\varepsilon(\boldsymbol{E}\cdot\boldsymbol{n})\boldsymbol{n}. \tag{A3}$$

Due to the continuity conditions at the interfaces, we have $D_z=0$. Eliminating then D_x, E_x and E_z from these three equations, we easily calculate $(\partial\Phi/\partial z)$ and deduce Eq. (13):

$$\delta_{\mathrm{calc}}=\int_{-d/2}^{d/2}\left(\frac{n_0 n_e}{\sqrt{n_0^2\sin^2\theta+n_e^2\cos^2\theta}}-n_0\right)dz\,.$$

[1] B. Jérôme, Rep. Prog. Phys. **54**, 391 (1991).
[2] F. Cognard, Mol. Cryst. Liq. Cryst. **1**, 1 (1982).
[3] M. G. Tomilin, J. Opt. Technol. **64**(5), 452 (1997).
[4] H. Yokoyama, Mol. Cryst. Liq. Cryst. **165**, 265 (1988).
[5] A. Ishizaki, H. Abe, N. Ando, Y. Imura, and S. Kobayashi, Mol. Cryst. Liq. Cryst. **258**, 277 (1995).
[6] V. P. Vorflusev, H. S. Kitzerow, and V. G. Chigrinov, Appl. Phys. A: Mater. Sci. Process. **64**, 615 (1997).
[7] Y. Imura, N. Kobayashi, and S. Kobayashi, Jpn. J. Appl. Phys. **34**, 1935 (1995).
[8] E. Polossat, I. Dozov, Mol. Cryst. Liq. Cryst. **282**, 223 (1996).
[9] J. S. Patel, T. M. Leslie, and J. W. Goodby, Ferroelectrics **59**, 137 (1984).
[10] D. Williams and L. E. Davis, J. Phys. D **19**, L37 (1986).
[11] P. Hubert, H. Dreyfus, D. Guillon, and Y. Galerne, J. Phys. II **5**, 1371 (1995).
[12] L. T. Creagh and A. R. Kmetz, Mol. Cryst. Liq. Cryst. **24**, 58 (1973).
[13] F. J. Kahn, Appl. Phys. Lett. **22**, 386 (1973).
[14] S. Faetti, M. Gatti, V. Palleschi, and T. J. Sluckin, Phys. Rev. Lett. **55**, 1681 (1985).
[15] B. Jérôme, P. Pieranski, and M. Boix, Europhys. Lett. **5**, 693 (1988).
[16] M. Monkade, M. Boix, and G. Durand, Europhys. Lett. **5**, 697 (1988).
[17] M. Monkade, P. Martinot-Lagarde, G. Durand, and C. Granjean, J. Phys. II **7**, 1577 (1997).
[18] U. Kuhnau, A. G. Petrov, G. Klore, and H. Schmiedel, Phys. Rev. E **59**, 578 (1999).
[19] P. Hubert and Y. Galerne, Appl. Phys. Lett. **71**, 1050 (1997).
[20] Y. Galerne and P. Hubert Eur. Phys. J. B **8**, 245 (1999).
[21] J. G. Fonseca, P. Charue, and Y. Galerne, Mol. Cryst. Liq. Cryst **329**, 597 (1999).
[22] R. Barberi, G. Durand, Appl. Phys. Lett. **58**, 2907 (1991).
[23] R. Barberi, M. Giocondo, and G. Durand, Appl. Phys. Lett. **60**, 1085 (1992).
[24] R. Barberi, M. Giocondo, Ph. Martinot-Lagarde, and G. Durand, Appl. Phys. Lett. **62**, 3270 (1993).
[25] I. Dozov, M. Nobili, and G. Durand, Appl. Phys. Lett. **70**, 1179 (1997).
[26] P. G. de Gennes and J. Prost, *The Physics of Liquid Crystals* (2nd ed. Clarendon, Oxford, 1993).
[27] D. Rivière, Y. Lévy, and E. Guyon, J. Phys. (France) Lett. **40**, L-215 (1979).
[28] G. Barbero, R. Barberi, J. Phys. (Paris) **44**, 609 (1983).
[29] G. Barbero, N. V. Madhusudana, and G. Durand, J. Phys. (France) Lett. **45**, L-613 (1984).
[30] S. Naemura, Appl. Phys. Lett. **33**, 1 (1978).
[31] T. Motooka, A. Fukuhara, and K. Suzuki, Appl. Phys. Lett. **34**, 305 (1979).
[32] S. Naemura, J. Phys. (Paris), Colloq. **40** (C3), 515 (1979).
[33] K. H. Yang and C. Rosenblatt, Appl. Phys. Lett. **43**, 62 (1983).
[34] C. Rosenblatt, J. Phys. (Paris) **45**, 1087 (1984).
[35] J. Sicart, J. Phys. (France) Lett. **37**, L-25 (1976).
[36] P. Chiarelli, S. Faetti, and L. Fronzoni, Phys. Lett. **101A**, 31 (1984).
[37] S. Faetti and V. Palleschi, J. Phys. (France) Lett. **45**, L-313 (1984).
[38] K. H. Yang, J. Appl. Phys. **53**, 6742 (1982).
[39] H. A. Van Sprang and R. G. Aartsen, Mol. Cryst. Liq. Cryst. **123**, 355 (1985).
[40] H. Yokoyama and H. A. Van Sprang, J. Appl. Phys. **57**, 4520 (1985).
[41] H. Yokoyama, S. Kobayashi, and H. A. Van Sprang, J. Appl. Phys. **61**, 4501 (1987).
[42] S. Faetti, M. F. Gatti, and V. Palleschi, J. Phys. (France) Lett. **46**, L-881 (1985).
[43] S. Faetti and V. Palleschi, Liq. Cryst. **2**, 261 (1987).
[44] M. Nobili and G. Durand, Phys. Rev. A **46**, R6174 (1992).
[45] D. F. Gu, S. Uran, and C. Rosenblatt, Liq. Cryst. **19**, 427 (1995).
[46] D. Subacius, V. M. Pergamenshchik, and O. D. Lavrentovich, Appl. Phys. Lett. **67**, 214 (1995).
[47] M. Nobili, Ph.D. Thesis, University of Pisa, Italy, 1992.
[48] V. Frederiks and V. Zolina, Trans. Faraday Soc. **29**, 919 (1933).
[49] A. Rapini and M. Papoular, J. Phys. (Paris), Colloq. **30**, 54 (1969).
[50] H. Yokoyama, Phys. Rev. E **55**, 2938 (1997).
[51] G. Barbero and S. Ponti, Phys. Lett. A **239**, 267 (1998).
[52] I. Dozov, G. Barbero, J. F. Palierne, and G. Durand, Europhys. Lett. **1**, 563 (1986).
[53] J. C. Wittman and P. Smith, Nature (London) **352**, 414 (1991).

[54] G. P. Chen, H. Takezoe, and A. Fukuda, Liq. Cryst. **5**, 241 (1989).
[55] D. A. Dunmur, M. R. Manterfield, W. H. Miller, and J. K. Dunleavy, Mol. Cryst. Liq. Cryst. **45**, 127 (1976).
[56] S. Sen, P. Brahma, S. K. Roy, D. K. Mukherjee, and S. B. Roy, Mol. Cryst. Liq. Cryst. **100**, 327 (1983).
[57] L. A. Karamysheva, E. I. Kovshev, A. I. Pavluchenko, K. V. Roitman, V. V. Titov, S. I. Torgova, and M. F. Grebenkin, Mol. Cryst. Liq. Cryst. **67**, 241 (1981).
[58] M. J. Bradshaw, E. P. Raynes, J. D. Bunning, and T. E. Faber, J. Phys. (Paris) **46**, 1513 (1985).
[59] P. R. Maheswara, V. A. Raghunathan, and N. V. Madhusudana, Liq. Cryst. **14**, 483 (1993).
[60] G. Barbero and R. Bartolino, Physica B **119**, 229 (1983).
[61] H. V. Kanel, J. D. Litster, J. Melngailis, and H. I. Smith, Phys. Rev. A **24**, 2713 (1981).
[62] S. Murakami, H. Naito, and M. Okuda, Mol. Cryst. Liq. Cryst. **263**, 2411 (1995).
[63] M. Brunet-Germain, C. R. Hebd. Seances Acad. Sci., Ser. B **271**, 1075 (1970).
[64] G. Lester, J. Hammer, and H. Coles, J. Chem. Phys. **103**, 9053 (1995).